

SCO X-1: HINTS OF PERIODIC VARIABILITY AT RADIO FREQUENCIES

C. F. BRADSHAW¹ AND B. J. GELDZAHLER

Institute for Computational Sciences and Informatics, Center for Earth Observing and Space Research, George Mason University,
Fairfax, VA 22030; cbradsha@mitre.org, bgeld@erols.com

AND

E. B. FOMALONT

National Radio Astronomy Observatory, Charlottesville, VA 22903; efomalon@sru.cv.nrao.edu

Received 1996 July 5; accepted 1996 December 5

ABSTRACT

We present the results of the flux density variability observations of Sco X-1 obtained during six VLA observing sessions between 1981 and 1990. The light curves indicate three timescales of flux density variation: slow, intermediate, and rapid. The rapidity of the variations sets a conservative upper limit on size of ~ 6 mas, assuming a distance of 200 pc, from light travel arguments for the radio-emitting regions. The corresponding brightness temperature of greater than 10^7 K indicates a nonthermal origin for the radio emission. A detailed analysis of the light curves suggests that the radio emission may exhibit true periodicity on timescales of ~ 3 hr. We also provide a prescription for accurate signal recovery and image restoration of point and extended sources when an object of varying signal is present in the synthesized beam.

Subject headings: radiation mechanisms: nonthermal — radio continuum: stars — stars: individual Scorpius X-1

1. INTRODUCTION

Sco X-1 is the brightest nonsolar X-ray source in the sky, located an estimated 200–2000 pc from the Sun at a Galactic latitude of $+25^\circ$. Sco X-1 was quickly identified with an optical star that was found to be a binary star. The orbital period (0.787 days) was derived by Cowley & Crampton (1975) from spectroscopic observations of He II ($\lambda 4686$) radial velocities, but the normal star's spectral luminosity classification has been uncertain because of the hot X-ray source heating the normal star's atmosphere. Observations soon after the original discovery quickly demonstrated that Sco X-1 is a highly variable X-ray source and that the variations are independent of the binary orbital period (Priedhorsky & Holt 1987). Following the discovery of radio emission from Sco X-1 (Ables 1969; Braes & Miley 1971), Hjellming & Wade (1971) showed that this emission also varied sporadically and dramatically.

For 20 years, precision astrometric observations of Sco X-1 were obtained in hopes that the source could be shown to be a microquasar. With lobe motion relative to the central engine validating the Blandford & Rees (1974) model, a new level of model detail could be pursued. The results of using Sco X-1 as a probe to test the kinematic aspect of the dual beam model have been published elsewhere (Fomalont & Geldzahler 1991). In brief, we found that Sco X-1 is, in fact, *not* a scaled down version of an extragalactic double radio source; the apparent lobes are stationary in the sky and are background extragalactic objects.

Determining the precise positions of the Sco X-1 “lobes” mandated that we remove the effects of radio variability from the binary system. A tacit assumption of interferometry is that the source does not vary during the aperture synthesis observations, and failure to remove the star-like features produced by variability around Sco X-1 during the CLEANing process prevented accurate determination of the positions of the other sources in the synthesized beam.

In this paper, we present the light curves of Sco X-1 during our VLA observations and their implications for the physical parameters of the underlying system. First, we briefly describe our set of observations. We next provide a procedure to obtain accurate astrometric positions of objects when a source in the synthesized beam varies during the observations. The recovered light curves for each observing epoch and frequency are then presented. Finally, we use the light curves to derive a timescale of variation in the emission, infer some of the binary physical characteristics, and compare our results with other published data.

2. OBSERVATIONS

We obtained data at six epochs of A-configuration VLA observation. Nearly identical (u, v)-plane coverage was used for each set of observations to minimize systematic errors when flux densities measured at different epochs were compared. The flux densities were tied to the calibrator 3C 286 to an accuracy of 1%. 3C 286 has no history of flux density variation greater than 4% over the last 15 years.

Radio maps were made for each epoch using the 1990 October 15 version of AIPS (the most recent version after our last observing epoch) to minimize systematic errors that could arise from using software that was not uniform. AIPS software was used to make and CLEAN the maps, and one iteration of self-calibration was found to be sufficient to remove tropospheric fluctuations and reach the expected signal-to-noise ratios.

The core varied significantly during the observations for each epoch. This variability was removed by (i) dividing the observations into sufficiently short time segments to eliminate variations within the segments, (ii) mapping each segment and removing the core, (iii) combining the maps with only the “lobes,” and (iv) removing the “lobes” from the u - v data, leaving only the variable core. These core data, after removal of Sco X-1's “lobes,” were averaged over 10 minute intervals and plotted to produce the light curves in Figures 1–6 for epochs 1981–1985 and 1990, respectively.

¹ Also at MITRE Corporation, McLean, VA 22102.

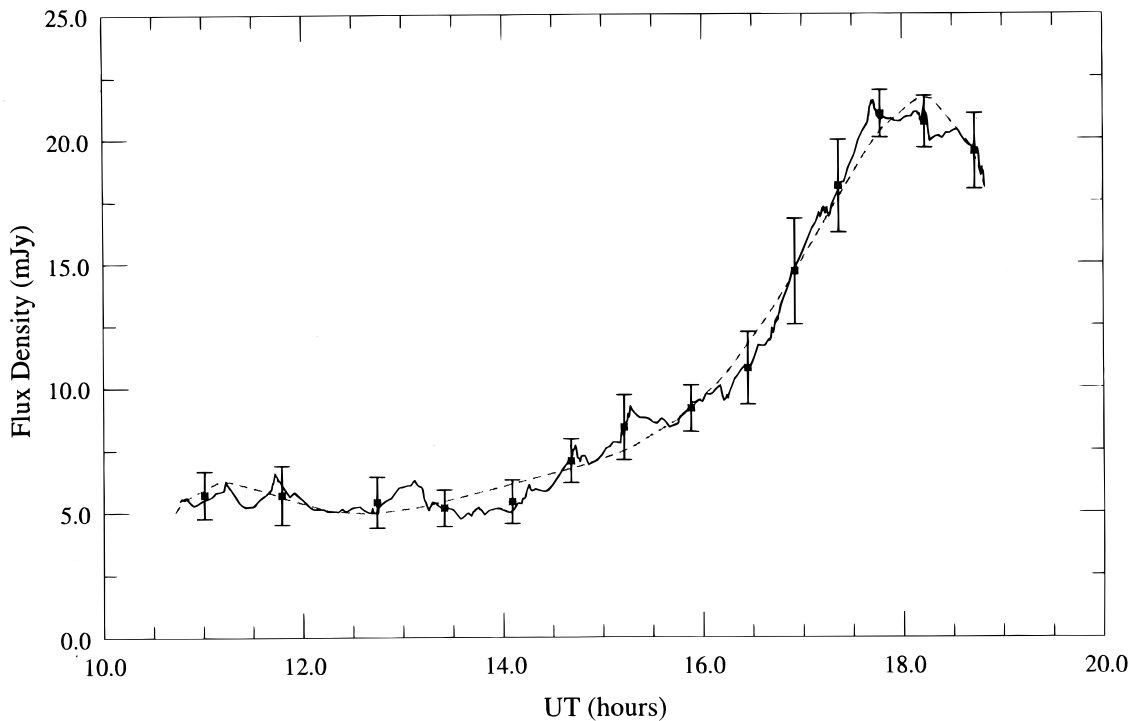


FIG. 1.—1981 Sco X-1 6 cm light curve (10 minute average) with polynomial fit (10 point window moving average with integration time 20 s per sample).

3. Sco X-1 VARIABILITY

VLA A-configuration radio data of Sco X-1 obtained during 1981–1985 and 1990, listed in Table 1, were analyzed for periodic or quasiperiodic variability with periods of 1–4

hr. The data in epochs 1981, 1982, 1984, 1985, and 1990 suggest overlapping outbursts of radio emission. Time segments in all epochs except 1983 incorporate slow, intermediate, and rapid flux density changes. An exponential form

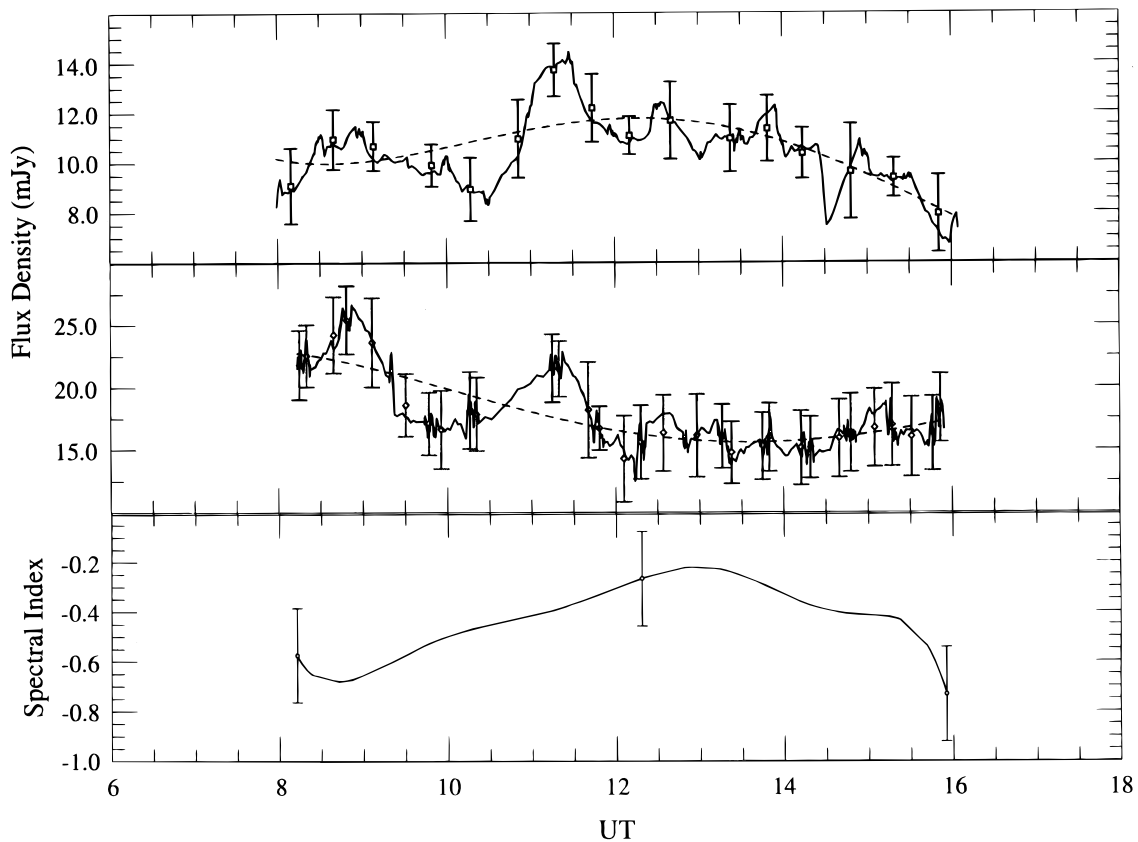


FIG. 2.—(a) 1982 Sco X-1 6 cm light curve (10 minute average) with polynomial fit (10 point window moving average with integration time 20 s per sample). (b) 1982 Sco X-1 20 cm light curve (10 minute average) with polynomial fit (10 point window moving average with integration time 20 s per sample). (c) 1982 Sco X-1 spectral index. The 2σ error bar equals 0.38.

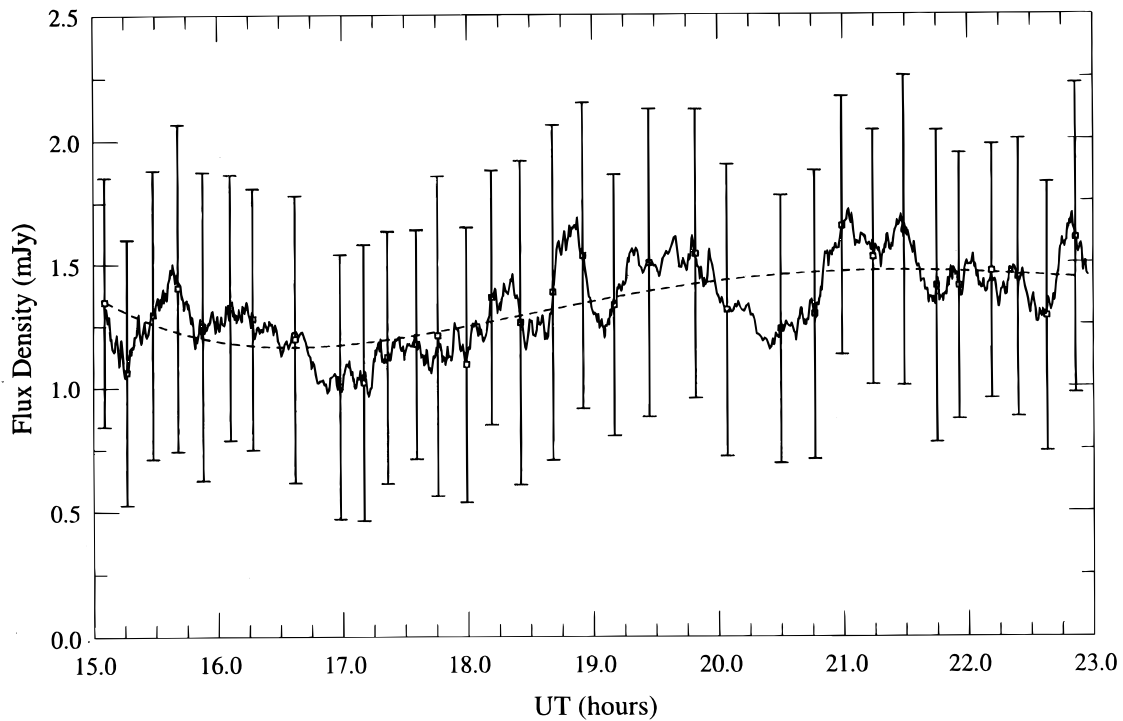


FIG. 3.—1983 Sco X-1 6 cm light curve (10 minute average) with polynomial fit (10 point window moving average with integration time 30 s per sample).

$S_0 e^{at}$ (where t is given in hr, a is the time constant in hr^{-1} , and S_0 is the flux density at the start of the exponential rise) was assumed for the bursts because the exponential provided a better fit to the data during these events than a linear form.

3.1. 1981.098

Figure 1 shows a 5 minute moving average of the CLEANed flux density as a function of time. The obser-

vations spanned 10 minutes at 6 cm and 10 minutes at 20 cm and included 20 minute amplitude calibrations to tie the flux densities to 3C 286. The 1981 flux density remained relatively constant at 5 mJy for approximately 3 hr, increased steadily for 1.5 hr to 8 mJy, remained steady at 8 mJy for 1 hr, rose with an exponential time constant equal to 0.36 ± 0.16 over the next 2 hrs, peaking at 22 mJy, and then began a decline during the last observation hour to about 17 mJy.

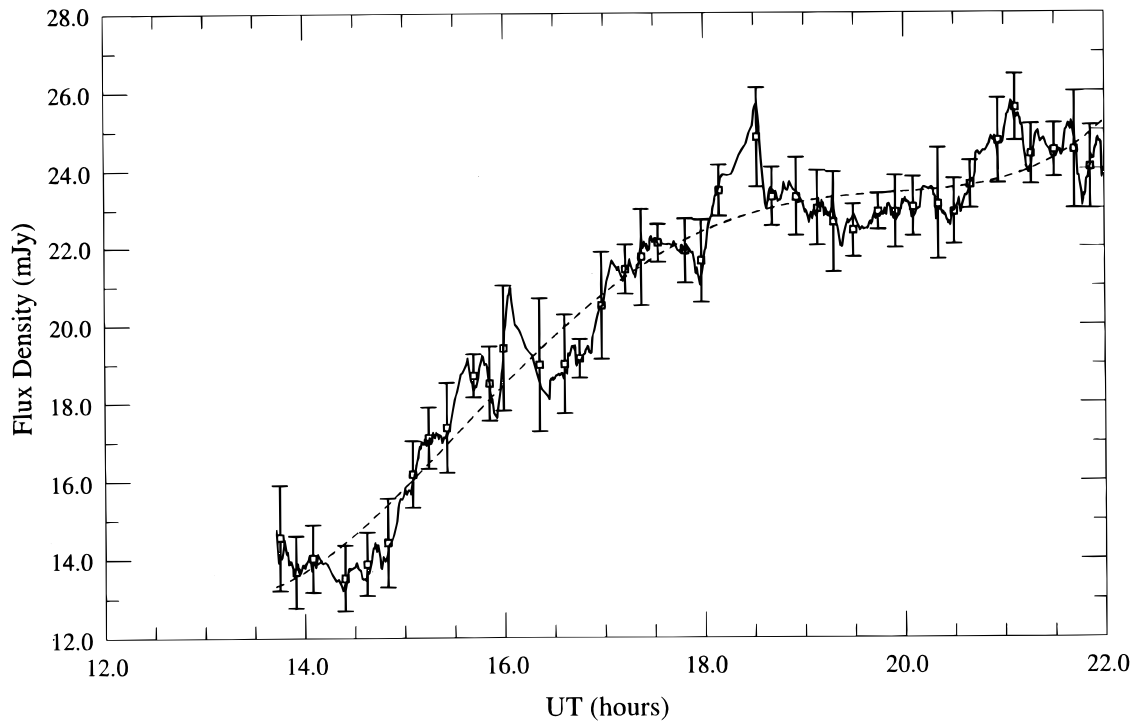


FIG. 4.—1984 Sco X-1 6 cm light curve (10 minute average) with polynomial fit (10 point window moving average with integration time 30 s per sample).

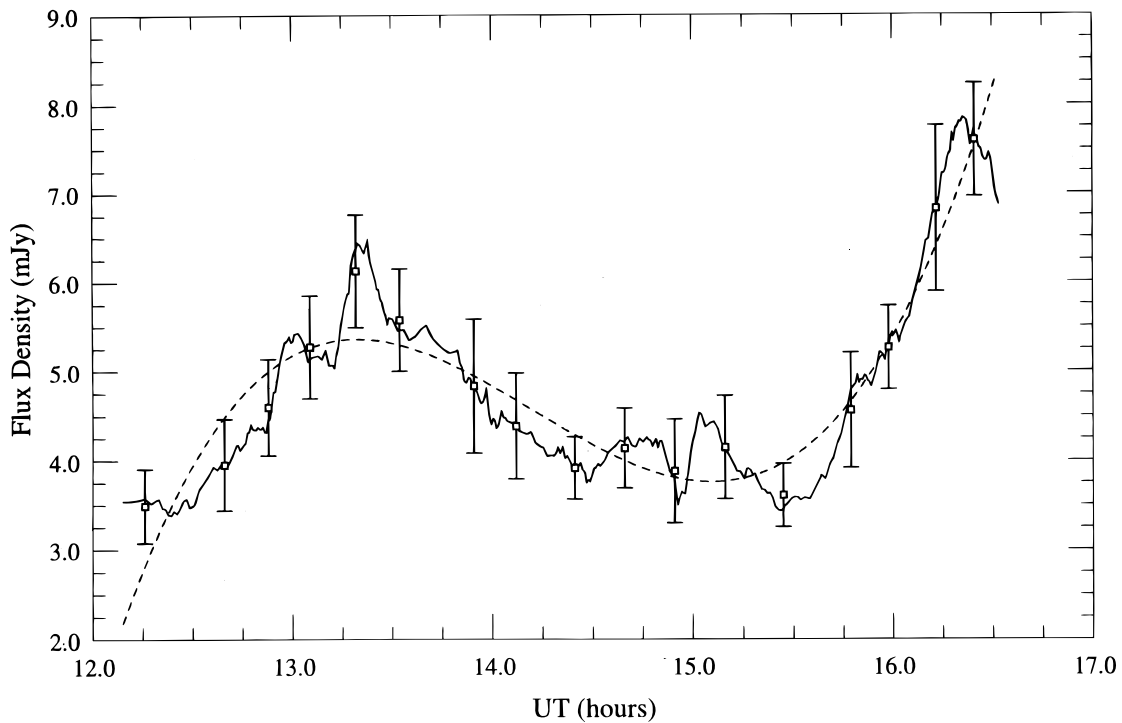


FIG. 5a

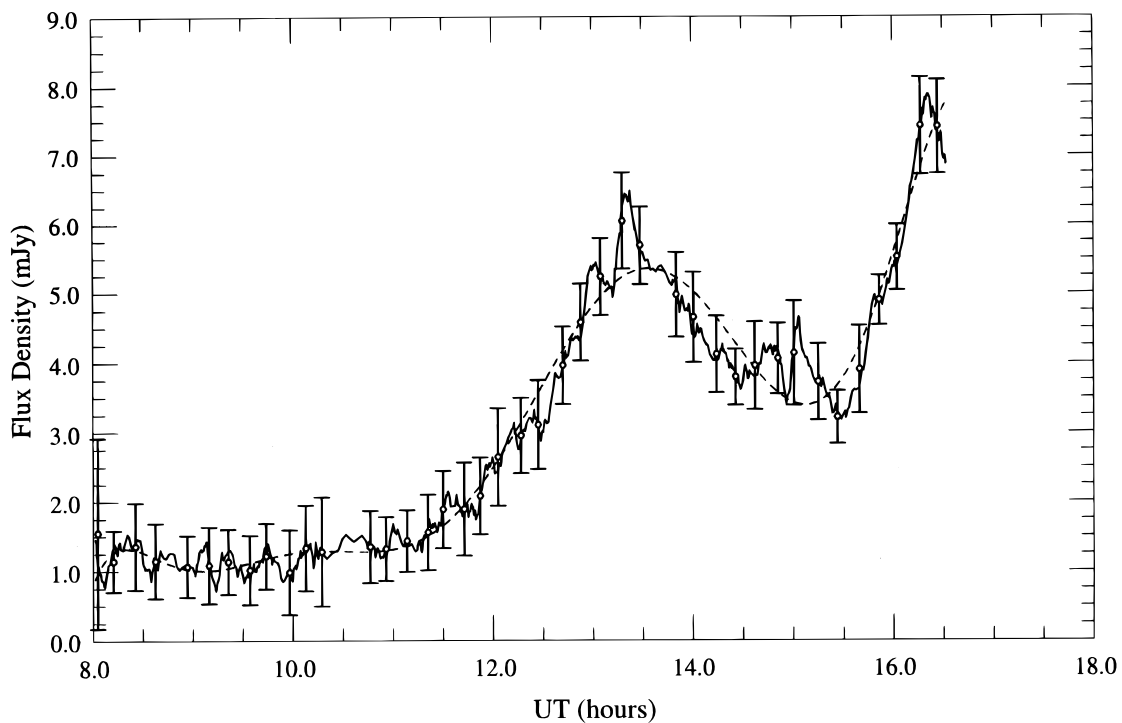


FIG. 5b

FIG. 5.—(a) 1985 Sco X-1 6 cm light curve (10 minute average) with polynomial fit (10 point window moving average with integration time 30 s per sample). (b) 1985 Sco X-1 6 cm light curve (10 minute average) with polynomial fit of order 10 with all data points included.

3.2. 1982.212

Figures 2a and 2b show 5 minute moving averages of both the 6 and the 20 cm 1982 data. The 20 cm data observations alternated with the 6 cm observations. The observations contained 20 minute amplitude calibration gaps. The 1982 6 cm flux density varied from 6 to 16 mJy and averaged 10 mJy. About 2.5 hr into the observation, a

flaring event occurred during which the flux density made a discontinuous jump from approximately 8 mJy to 12 mJy. Three hours into the observation, the flux density peaked at 14 mJy, then steadily declined to 6 mJy over the remaining 5 hr. The 1982 20 cm flux density decreased from about 25 mJy to around 17 mJy during the first 2.5 observation hours. It then increased to almost 20 mJy 2.5–3.5 hr into the

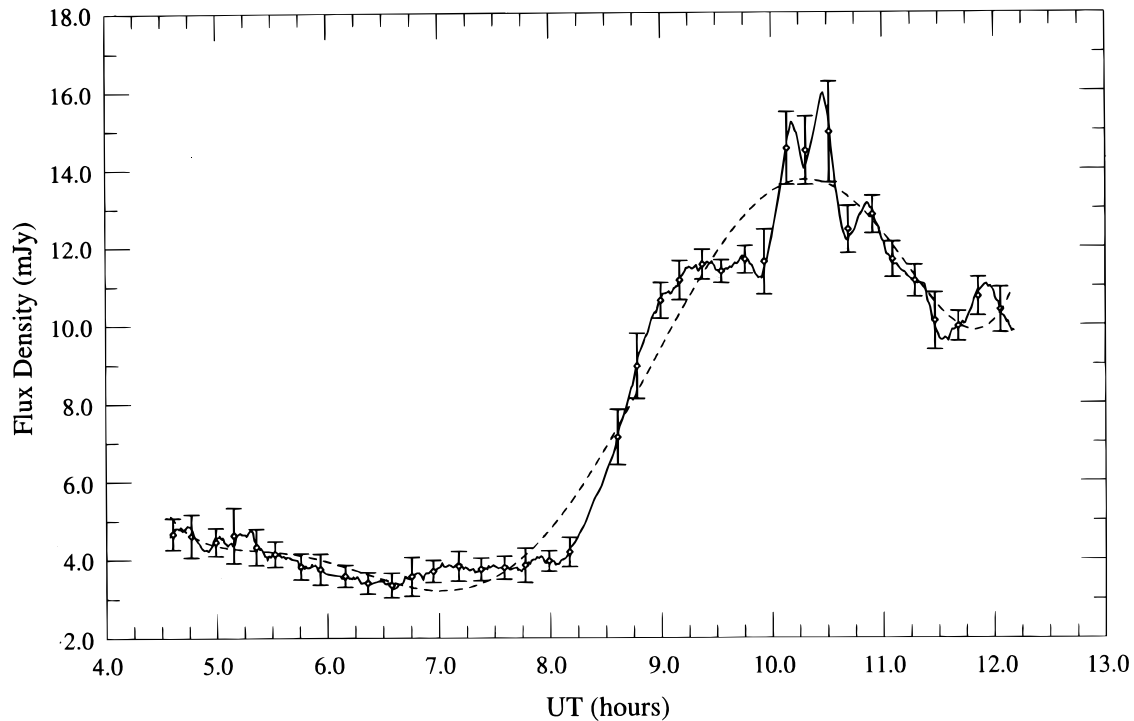


FIG. 6a

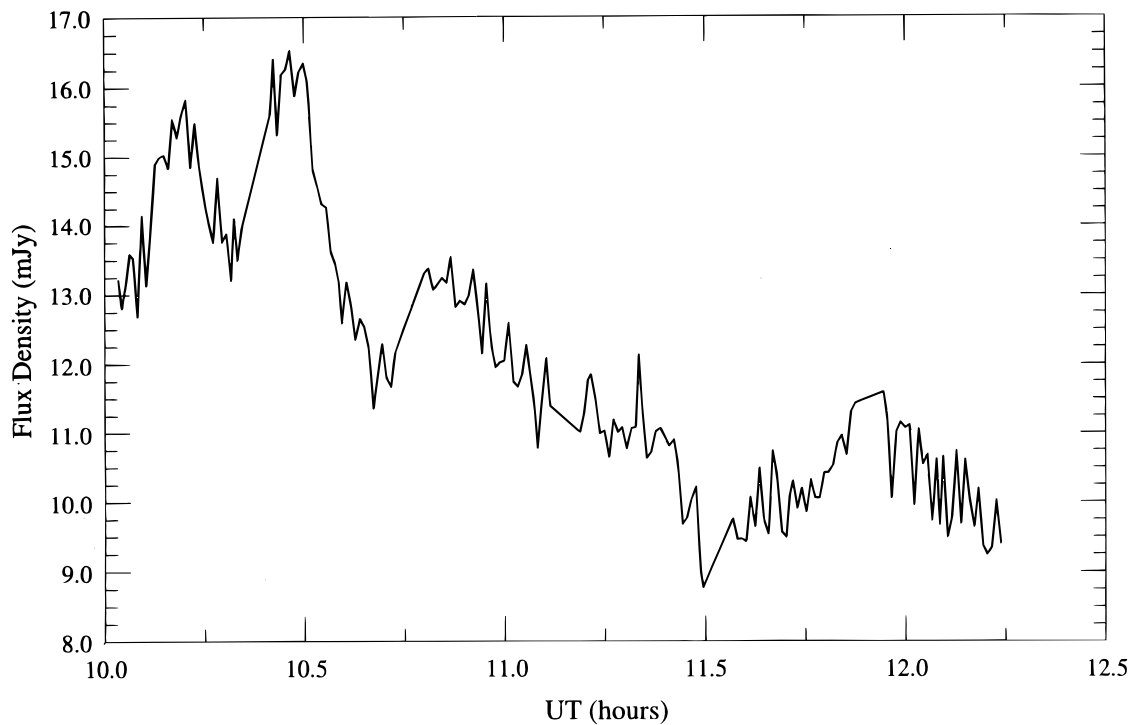


FIG. 6b

FIG. 6.—(a) 1990 Sco X-1 6 cm light curve (10 minute average) with polynomial fit (10 point window moving average with integration time 40 s per sample). (b) 1990 Sco X-1 6 cm light curve expansion of rapid variation time.

observation. The remaining 4.5 hr of observation showed the flux density dropping to 17 mJy in ~ 0.5 hr and thereafter remaining nearly constant. The increase of the 20 cm flux density at 3.5 hr into the observation coincided with or lagged slightly behind the 6 cm flux density increase.

The spectral index of the 1982 data (Fig. 2c) varied between -0.67 and -0.18 . During the first hour of the observation, both the 6 cm and 20 cm flux densities

increased. The 6 cm and 20 cm flux densities showed the same percentage increase, but because of the larger 20 cm flux density the resulting spectral index dropped to -0.67 . From hours 9 through 10.5, the 20 cm flux density decayed from a peak of 25 mJy to about 15 mJy, while the 6 cm flux density decayed from about 10 to 9 mJy. The more rapid decay of the 20 cm flux density resulted in the spectral index flattening from -0.68 to about -0.5 . At hours 9–10.5, an

TABLE 1
SCO X-1 6 CM EXPERIMENTAL DATA

Year	Number of Samples	Observation Time (hr)	Integration Time (per sample)
1981.....	551	8.14	20
1982.....	551	8.16	20
1983.....	1124	8.13	20
1984.....	822	8.35	30
1985.....	826	8.68	30
1990.....	594	7.72	40

increase in the 6 cm flux density to about 10 mJy and the 20 cm flux density to about 20 mJy resulted in a slow flattening of the spectral index to about -0.3 . The more rapid decay of the 20 cm flux density from the intermediate peak during the next hour resulted in the spectral index peaking at -0.18 at hour 13. During the remainder of the observing epoch, the 6 cm flux density decayed slowly to 5 mJy, while the 20 cm flux density slowly increased to about 15 mJy. The result was that the spectral index decreased to -0.5 . The sharp decrease at the end of the observation epoch is an artifact of the analysis and therefore is not physically meaningful.

Because the 6 cm and 20 cm flux density data were taken in alternate 10 minute intervals, the spectral index was derived by fitting seventh-order polynomials (the highest order possible without numerical underflow using 32-bit computations) to the 6 and 20 cm flux density data, resampling the polynomials to obtain simultaneous least mean square estimates, and calculating the spectral index from the resampled values. This method gives an estimate of the average spectral index of the flux density over the 20 minute observing cycle, but misses any rapid fluctuations that occurred within the 10 minute alternating sample times when no data were taken.

3.3. 1983.910

The 1983 flux density remained constant but averaged less than 2 mJy throughout the entire observing period. Figure 3 shows the 5 minute moving average of these data. The radio emission from Sco X-1 was essentially shut off during this epoch and the low signal-to-noise ratio of the 1983 data precluded finding any significant period or any insights about variability.

3.4. 1984.964

The 1984 flux density (Fig. 4) exhibited significant short-term variations while increasing from an initial 14 mJy to a final 26 mJy. There were small (about 3–4 mJy) flares at 16 and 18 hr UT, and from 18 to 22 hr UT the flux density appeared to dip slightly (~ 2 mJy) and recover. Between 14.5 and 15.9 hr UT in Figure 4, the flux density rose with an exponential time constant of 0.30 ± 0.06 . From 16 to 18 hr UT, the flux density rose with an exponential time constant of 0.12 ± 0.06 .

3.5. 1985.183

Figure 5a shows the cleaned 5 minute moving average of the 1985 6 cm flux density as a function of time, and Figure 5b shows the data before cleaning. The flux density was constant at 1 mJy for 3 hr after the start of the observation, and the data were discarded because the signal-to-

noise ratio was too low and the phase information reflected that there was no appreciable signal above receiver noise. We inferred that there was insufficient information for making a reasonable estimate of changes in the flux density. Beginning at hour 4, the flux density increased, with an exponential time constant of 0.65 ± 0.12 , to 6 mJy during the next 2.5 hr. It then decayed (exponential time constant equal to -0.43 ± 0.12) to 4 mJy over the next hour. Subsequently, the flux density remained constant for about 1 hr before increasing exponentially (time constant equal to 1.03 ± 0.10) again to 8 mJy within about 0.5 hr. During the last 0.5 hr of observations, the flux density appeared to be decreasing, but this result is uncertain.

3.6. 1990

The observation (Figs. 6a and 6b) showed more flaring activity than any other epoch and therefore provides significant insight into physical processes in the Sco X-1 system. However, due to rapid flaring in the 6 cm 1990 flux density, there was no single polynomial, to order 11, that provided a good fit to the flux density over the observing interval. The flux density changes described below were calculated as piecewise linear regression fits to the natural log of the flux density in designated time segments. The 1990 flux density averaged 4 mJy for 4 hr before increasing (exponential time constant equal to 1.2 ± 0.06) within 1 hr to 11 mJy. The flux density then maintained an average of 11 mJy with rapid and short duration (~ 0.1 hr) flares superimposed. The data points have been connected by lines in Figure 6b after 9.9 hr (UT) to better illustrate the rapidity of the flares. The decay between UT 10.8 and 11.2 hr had an exponential time constant of $\sim 0.6 \pm 0.03$. This variation in the 1990 flux density prevented frequency analysis for the search periods; however, the rapid flaring provided an upper limit on the emission size, from speed-of-light arguments, of approximately 10^{14} cm (assuming 200 pc distance to the object; Fomalont & Geldzahler 1991).

Table 2 provides the variability time constants for each epoch and the upper limits on the source sizes derived from speed-of-light arguments (Marscher et al. 1979). The fitted

TABLE 2
FLUX DENSITY VARIATIONS AND PHYSICAL SIZE

EPOCH	FITTED TIME CONSTANT (hr ⁻¹)	DETERMINATION TIMES (UT)	UPPER LIMIT ON SIZE ^a	
			(mas)	(10 ¹⁴ cm)
1981.....	0.36 ± 0.16	13.7–15.2	309	9.2
	0.57 ± 0.07	16.2–17.7	195	5.8
1982.....	0.53 ± 0.11	10.5–11.5 (6 cm)	154	4.6
	0.23 ± 0.16	10.3–11.3 (20 cm)	322	9.6
1984.....	0.30 ± 0.06	14.5–15.9	321	9.6
1985.....	0.65 ± 0.12	12.4–13.3	103	3.1
	-0.43 ± 0.12	13.3–14.5	207	6.2
	1.03 ± 0.10	15.6–16.3	50	1.5
1990.....	1.2 ± 0.06	8.1–8.9	49	1.5
	1.3 ± 0.04	9.9–10.2	17	0.5
	-1.1 ± 0.03	10.2–10.3	7	0.2
	1.3 ± 0.04	10.3–10.4	6	0.2
	-1.6 ± 0.03	10.4–10.7	14	0.4
	1.0 ± 0.03	10.7–10.8	7	0.2
	-0.6 ± 0.03	10.8–11.2	49	1.5

^a Assuming 200 pc (Fomalont & Geldzahler 1991).

time constants result from a least-squares linear fit to the natural log of the flux densities. In all cases, we have assumed simple, exponentially expanding outbursts. We realize that this assumption is simplistic and that we have more likely observed the flux densities of two or more commingled outbursts. However, our representation provides a conservative measure of the upper limits of the source size. The outbursts are bounded by a source size upper limit of $r < 322 \text{ mas}$ ($9.6 \times 10^{14} [d/(200 \text{ pc}) \text{ cm}]$) and a source size upper limit of $r < 6 \text{ mas}$ ($0.2 \times 10^{14} [d/(200 \text{ pc}) \text{ cm}]$). The Sco X-1 system size is on the order of 10^{11} cm (Cowley & Crampton 1975).

4. HINTS OF PERIODIC EMISSION

We used Fourier transforms, Lomb-Scargle periodograms, and epoch-folding techniques to look for periodicity in the VLA data. Data from all epochs were filtered in the same manner for all methods by the following steps:

1. We determined which data were spurious. Examination of the phase data from each sample showed that at apparent low flux density levels the sample phases were random (i.e., noise-generated) and that at flux density levels with signal-to-noise ratios greater than 5 the sample phase approached zero (i.e., a real signal was present in the integrator). This provided a simple method of eliminating samples that consisted of little or no real signal. We then rejected any signal with a phase greater than 10° . All spurious amplitudes rejected were either the first or last sample of an observation period. The method also has the virtue of not systematically biasing the period search due to rejection of flaring or highly varying events.

2. Next, we removed secular trends from the data. The long-period mean variations were removed by fitting the data with a polynomial and subtracting the polynomial values at each sample time from the data. The polynomial order used to provide the best fit to the mean fluctuations was one less than the order at which the coefficient resulted in insignificant change. Fourth-order polynomials were used for 1981–1983 and 1984, fifth order for 1984, and seventh order for 1990 (the high order was required by the extreme flaring of the data; however, the data for this epoch still could not be properly normalized and was not used for period searches). We realize that by using high-order polynomials we may be removing part of the periodic activity that we seek and possibly adding spurious periodic activity, but by using this technique the high-frequency amplitudes produced by flux density flares are greatly reduced.

3. We next discarded outliers. The data at the beginning and end of a sample period, both before and after amplitude calibration, often showed large variations from the mean sample values. These large-amplitude changes were considered to be a spurious response of the system. Sample values greater than 3σ away from the mean sample value were considered outliers and deleted from the sample set. We recognize that this procedure is dangerous because we have no a priori way of knowing that these data are spurious.

Our search for rapid variations (1.7–50 mHz; 20 s to 10 minutes) used standard Fourier transform techniques. The data were binned, windowed, and the mean value subtracted. Several window functions were tried (Hanning, Hamming, and Blackman windows) with little or no difference in the transform results. The Blackman window was

used because of its slightly better resolution of nearby tones with significantly different amplitudes (Harris 1978).

The binned and windowed data from each epoch were transformed into the frequency domain using the fast Fourier Transform (FFT). Every 10 minute on-source interval contained approximately 30 samples; these on-source samples were placed in a matrix column, padded with zeros, and transformed into the frequency domain with the FFT. The resulting frequency data were then averaged to reduce the variance of the spectrum. This procedure is effectively the same as overlap and add techniques of spectral analysis, which could not be used because the samples were not continuous. This frequency search failed to find any significant periodic activity.

We also looked for slower variations (34 μHz –1.7 mHz; 10 minutes to 4 hr) by fitting trial data periods to the data to produce periodograms (Scargle 1982; Lomb 1976; Press & Rybicki 1989). The Lomb-Scargle periodogram is a period-search algorithm applicable when the data time-sampling is uneven. This algorithm also provides a statistical significance test of period probability within 1% under Gaussian noise conditions. However, because we cannot assume observations with Gaussian noise, we are uncertain of the true significance of the results. Therefore, the periodograms were only used to indicate trial periods, which were further tested by epoch folding.

The Lomb-Scargle periodograms were filtered to exclude frequencies greater than 10% of the Nyquist and window frequencies. A false periodogram of random samples, created with the data sampling windows, determined the window spectral leakage, or “window frequencies,” to be discarded.

Phase dispersion minimization (PDM) is a statistically correct method to search for and determine periodic activity (Davies 1990; Stellingwerf 1978). PDM require folding the data at a test period, binning the data, and developing a statistic from the bin variance and sample variance ratio. PDM approximately follows an F -distribution with $N - M$ and $N - 1$ degrees of freedom (Stellingwerf 1978), where M and N are the number of bins and samples, respectively. For large N , the PDM statistic accurately estimates the probability of a given period (Davies 1990). Figure 7 shows the PDM test results ($M = 10$) for epochs 1981, 1982, 1984, and 1985 for the 6 cm data.

In Figure 7, the PDM statistic ranges between 0 and 1. A value of 1 indicates that the variance of the period tested is the same as the sample variance (e.g., no period). The closer to zero the statistic lies for any period, the more unlikely it is that the period results from noise.

The 1981 PDM statistic showed two periods, one near 2.9 hr and one at 3.2 hr (the apparent doublet may be caused by beating with the 20 minute scan length). The period at 2.9 hr was chosen for epoch folding because its variance was slightly more distant from the sample variance than the 3.2 hr period. The 1982 PDM resulted in a broad range of periods between 2.5 and 3 hr. The smallest value of the test statistic, at 2.67 hr, was chosen for epoch folding. The 1984 PDM statistic clearly showed a best period at 2.86 hr, and this period was chosen for epoch folding. The 1985 statistic appears to have a broad range of periods at 2.9 hr. However, because the 1985 data filtering produced a total data time window near 6 hr with a flux density peak near the middle of the data, a 3 hr period is expected. This data truncation makes the period results, which appear to be

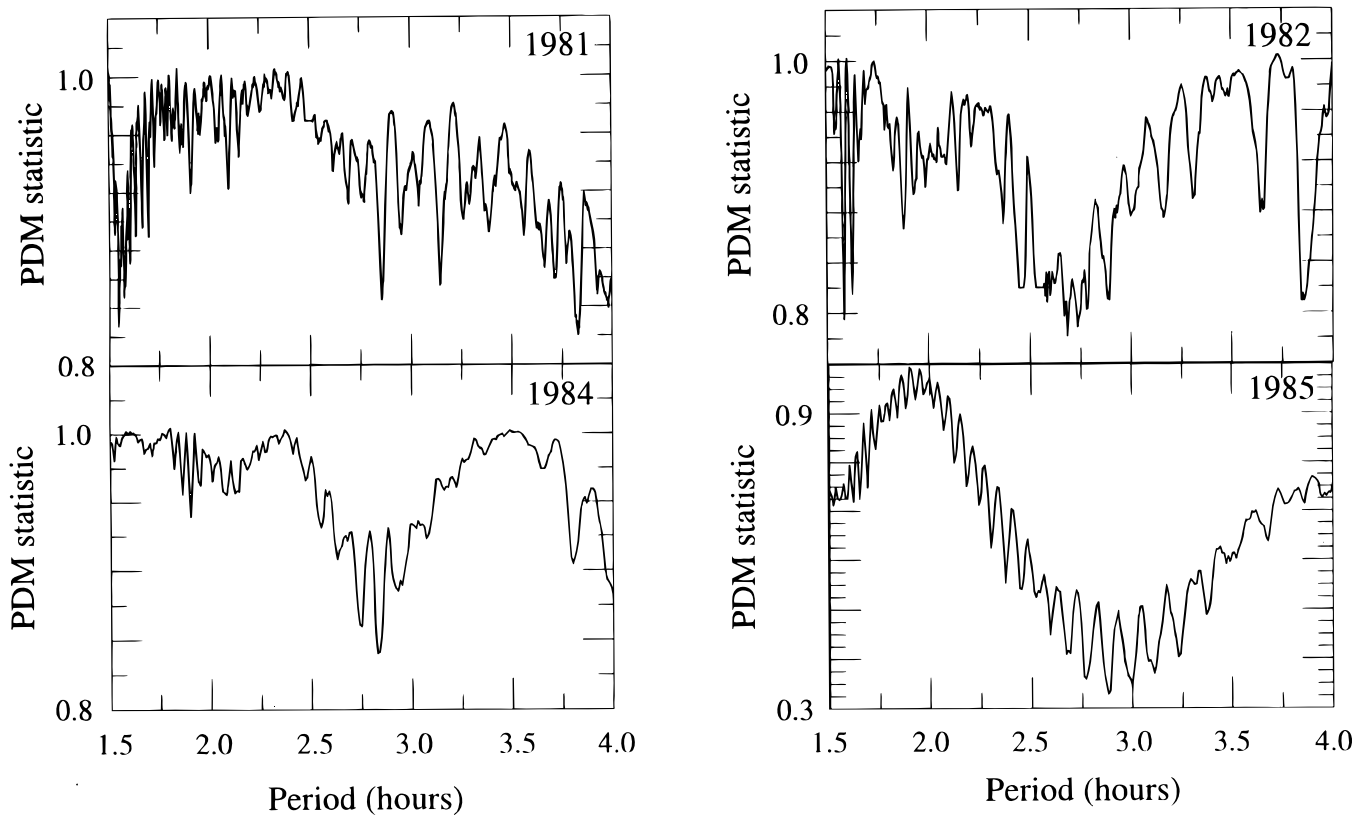


FIG. 7.—1984 Sco X-1 phase dispersion minimization (Stellingwerf 1978) results using the 6 cm radio flux density for epochs 1981, 1982, 1984, and 1985

more than 6σ different from random noise, suspect. We chose the period with the lowest value of the 1985 PDM statistic for epoch folding.

Figures 8–11 show the radio data folded at periods near 3 hr for epochs 1981, 1982, 1984, and 1985. Table 3 lists the

tested periods and the probability that the period is due to random fluctuations for each epoch. We assume that the flux density at each sample is independent and systematic errors (e.g., gain errors plus residual contamination from the “lobes”) are negligible. Such errors would result in

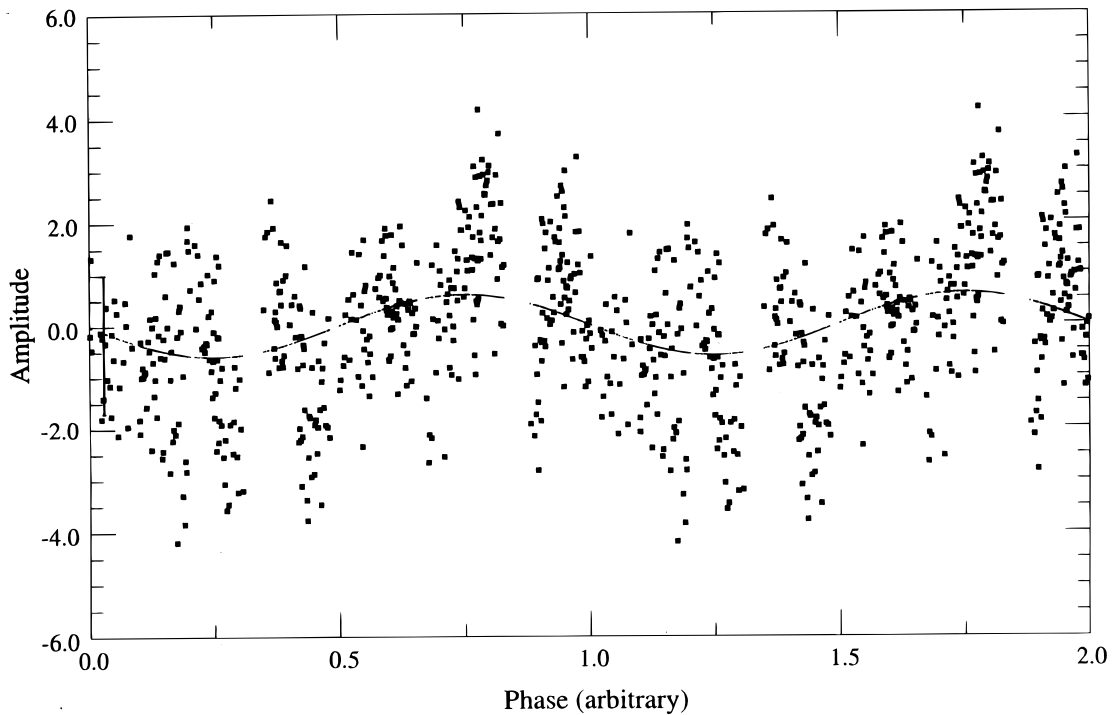


FIG. 8.—1981 Sco X-1 6 cm data folded at 2.86 hr

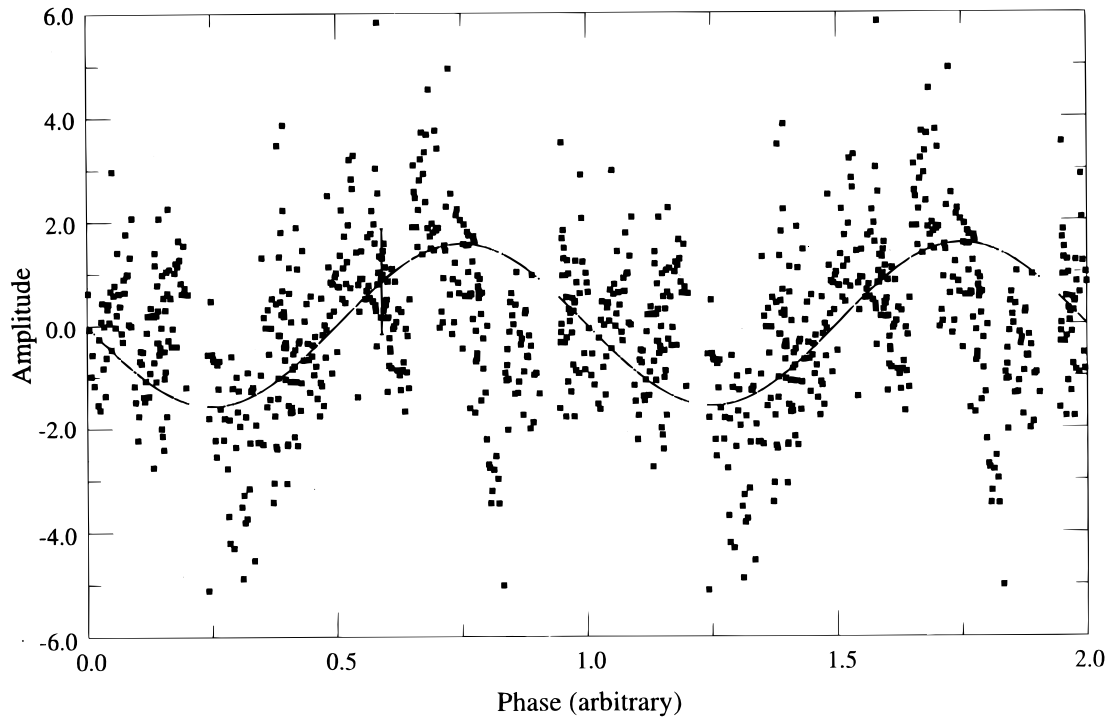


FIG. 9.—1982 Sco X-1 6 cm data folded at 2.69 hr

amplitude variations with timescales on the order of 10 minutes.

The 1985 folded data clearly show the 2.9 hr time interval between the flux density peaks of the 1985 light curve. Because the 1985 data are only 6 hr in length, the lack of more than two peaks diminishes the significance. In contrast, the other epochs span more than two complete period intervals. The combined 1981, 1982, 1984, and 1985 6 cm

data suggests that physical mechanisms within Sco X-1 are creating periodic radio emission with timescales of about 3 hr.

5. DISCUSSION

Assuming a 200 pc distance to the source (Fomalont & Geldzahler 1991) and a source angular diameter upper limit of 6 mas based on variability, the flux densities at the turn-

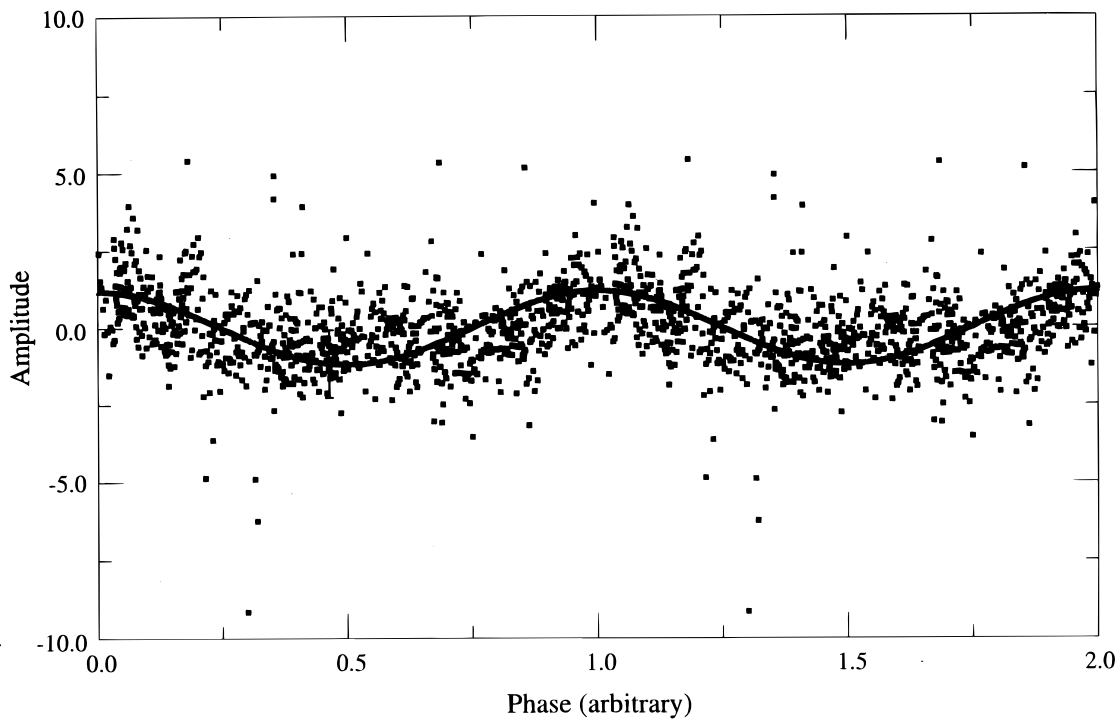


FIG. 10.—1984 Sco X-1 6 cm data folded at 2.83 hr

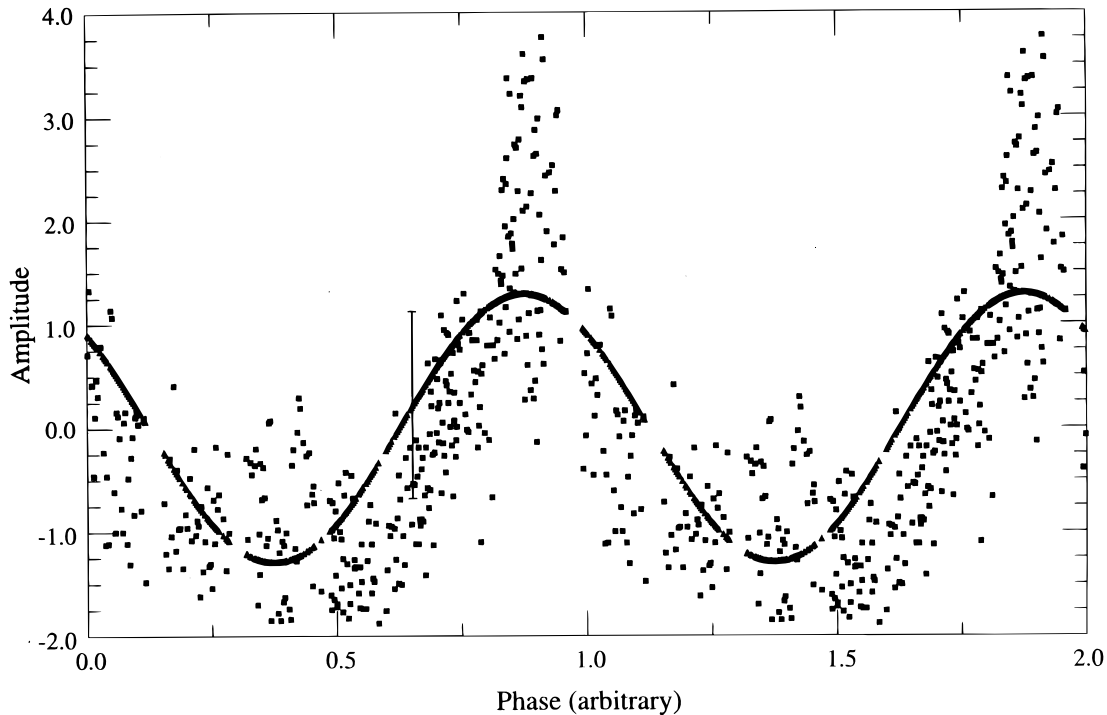


FIG. 11.—1985 Sco X-1 6 cm data folded at 2.9 hr

over frequency of 1 GHz (Velusamy, Pramesh, & Sukumar 1985; Geldzahler et al. 1983) are ≤ 15 mJy and ≤ 32 mJy for spectral indices of -0.18 and -0.67 (minimum and maximum in Fig. 2c), respectively. The peak brightness temperatures are $\geq 10^8$ K, indicating nonthermal emission.

Calculating from the exponential decay time constants described in the 1985 and 1990 6 cm flux density data and using the timescale for synchrotron losses $\tau_{\text{sync}} = 5.5 \times 10^8 B^{3/2} v^{-1/2}$ (Gregory 1972) results in a magnetic field strength $\sim 10^{-2}$ G. This field strength corresponds to a source angular size of 0.2 mas at a distance of 200 pc with a brightness temperature of 10^{11} K. Assuming a turnover frequency of 1 GHz and a cutoff frequency of 100 GHz, the energies contained in the magnetic field, E_m , and in the relativistic electrons, E_e , are 4.6×10^{29} and 5.6×10^{42} ergs, respectively. The total nonthermal radio luminosity is 10^{33} ergs s^{-1} .

Marscher & Brown (1975) described the 1972 Cyg X-3 radio flare flux density evolution with a variable spectral index arising from an expanding cloud of relativistic particles in a magnetic field. The model predicts a spectral index time evolution, with initial dominance by synchrotron energy loss that produce an exponential decay of radio flux densities and subsequent dominance of adiabatic losses that produce power-law energy losses. The flare decay in the

1985 and 1990 data and the evolution of the 1982 spectral index suggest a similar process for Sco X-1.

The spectral index evolution (Fig. 2c) suggests that our observations started during an adiabatic expansion phase of the radio-producing plasma that was followed by an injection of high-energy electrons. The particles stretch and carry the magnetic field, thereby producing the steeper spectral index with time. Although we do not have equivalent spectral indices for other epochs, the 1985 and 1990 light curves (Figs. 5 and 6) show an exponential rise and subsequent exponential decay that suggest similar energy injection and expansion processes. The calculated magnetic field strength and energy in relativistic electrons are comparable to those for Cygnus X-3.

There are three physical timescales associated with the Sco X-1 binary system: (i) periods associated with short-period emission like that expected from a rotating neutron star (seconds), (ii) variations close to the orbital period (1–19 hr), and (iii) supraorbital variability (more than 19 hr). Our data are sensitive only to (ii).

There is archival evidence suggesting 3 hr periods or events occurring on 3 hr timescales in both the radio (Hjellming et al. 1990) and optical (Severny & Kuvshinov 1975; Westphal, Sandage, & Kristian 1968; Cowley & Crampton 1975) Sco X-1 data. However, there are no optical observations overlapping with our observed radio periods. A 3 hr period from a 1.4 solar mass neutron star places the emission (or obscuring) material at a distance between $\sim 10^{10}$ and $\sim 10^{11}$ cm. How an interaction between this material and a neutron star could produce the observed periodic radio emission is unclear. Possible explanations include accretion flow shocks forming and dissipating regularly on timescales of a few accretion flow times (Fryxell & Taam 1988), a “hot spot” in the accretion disk precessing with the binary orbit, and a jet coupled with variations in accretion flow. The hot spot in the accretion

TABLE 3

PHASE DISPERSION MINIMIZATION RESULTS

Epoch	Period	Probability of Period Resulting from Noise
1981.....	2.86	3.1×10^{-2}
1982.....	2.69	5.7×10^{-4}
1984.....	2.83	1.3×10^{-2}
1985.....	2.9	$< 10^{-10}$

disk model is reminiscent of those needed for Lamb's quasi-periodic oscillation (QPO) beat frequency model (Priedhorsky et al. 1986).

6. CONCLUSIONS

We have found flux density variations in Sco X-1 that suggest 3 hr periods. These results were obtained as part of a program to monitor the radio morphology and measure the proper motion of Sco X-1 in which Fomalont & Geldzahler (1991) analyzed 10 years of accumulated 6 cm VLA observations. A detailed search for periodic flux density variations in the radio data suggests flux changes on timescales with periods between 2.5 and 3.5 hr (Bradshaw, Geldzahler, & Fomalont 1993). The presence of periodic variability at such a short-period suggests radio emission generated well within the binary orbit. The probability that the apparent periodicity in our Sco X-1 data is real is enhanced because it is seen under different flaring behaviors, integration times, and sampling windows in four different epochs, and also because we find approximate 3 hr timescales reported in previous optical and radio observations.

Our results are preliminary because the radio data is noisy, it is difficult to distinguish between flaring and periodic activity, the observations last only a few cycles of the 2.5–3.5 hr period, and the observations have sampling patterns that can produce spurious frequencies that mix with noise. Unfortunately, the observing sessions were too far apart in time to phase-connect the detected periods from epoch to epoch. VLA observations over several consecutive days might allow phase connection of similar data, which would be much more sensitive in the detection of 3 hr periods.

We thank the NRAO² director and staff who, over the years, have made this research possible by making observing time available and assisting in data reduction. We also thank P. Becker, P. Hertz, and M. Kafatos for helpful discussions.

² The National Radio Astronomy Observatory is a facility of the National Science Foundation operated under cooperative agreement by Associated Universities, Inc.

REFERENCES

- Ables, J. G. 1969, *Proc. Astron. Soc. Australia*, 1, 273
 Bradshaw, C., Geldzahler, B., & Fomalont, E. 1993, *BAAS*, 25, 1380
 Blandford, R., & Rees, M. 1974, *MNRAS*, 169, 395
 Braes, L., & Miley, G. K. 1971, *A&A*, 14, 160
 Cowley, A. P., & Crampton, D. 1975, *ApJ*, 201, L65
 Davies, S. 1990, *MNRAS*, 244, 93
 Fomalont, E. B., & Geldzahler, B. J. 1991, *ApJ*, 383, 289
 Fryxell, B., & Taam, R. 1988, *ApJ*, 335, 862
 Geldzahler, B. J., et al. 1983, *ApJ*, 273, L65
 Gregory, P. C. 1972, *Nature Phys. Sci.*, 239, 114
 Harris, F. 1978, *Proc. IEEE*, 66, 51
 Hjellming, R. M., et al. 1990, *ApJ*, 365, 681
 Hjellming, R. M., & Wade, C. M. 1971, *ApJ*, 158, L155
 Lomb, N. 1976, *A&SS*, 39, 447
 Marscher, A. P., Marshall, F. E., Mushotzky, R. F., Dent, W. A., Balonek, T. J., & Hartman, M. F. 1979, *ApJ*, 233, 498
 Press, W., & Rybicki, G. 1989, *ApJ*, 338, 277
 Priedhorsky, W., Hasinger, G., Lewin, W. H. G., Middleditch, J., Parmar, A., Stella, L., & White, N. 1986, *ApJ*, 306, L91
 Priedhorsky, W., & Holt, S. 1987, *ApJ*, 312, 743
 Scargle, J. 1982, *ApJ*, 263, 835
 Severny, A., & Kuvshinov, V. 1975, *ApJ*, 200, L13
 Stellingwerf, R. 1978, *ApJ*, 244, 953
 Velusamy, T., Pramesh, R., & Sukumar, S. 1985, *MNRAS*, 213, 735
 Westphal, J. A., Sandage, A., & Kristian, J. 1968, *ApJ*, 154, 139